Electronic Supplementary Material (ESI) for Energy Advances.

Supporting Information

Nickel Polyelectrolytes as Hole Transporting Materials for Organic and Perovskite Solar Cell Applications

Jin Hee Lee,[a] Kausar Ali Khawaja,[b] Faiza Shoukat,[b] Yeasin Khan,[a,c] Do Hui Kim,[d] Shinuk Cho,*[d] Bright Walker*[c], Jung Hwa Seo*[a]

[a]*Department of Physics, University of Seoul, Seoul, 02504,Republic of Korea*

[b]*Department of Physics, Dong-A University, Busan, 49315, Republic of Korea*

[c]*Department of Chemistry, Kyung Hee University, Seoul, 02447, Republic of Korea*

[e]*Department of Physics and Energy Harvest Storage Research Center (EHSRC), University of Ulsan, 44610, Ulsan, Republic of Korea*

Table S1. pH in solution measured in pH meters and Litmus

	pH (Litmus)	pH (pH meter)
Ni:PSS	7	6.82
Ni:PEDOT:PSS	2~3	2.48
PEDOT:PSS	1	2.04

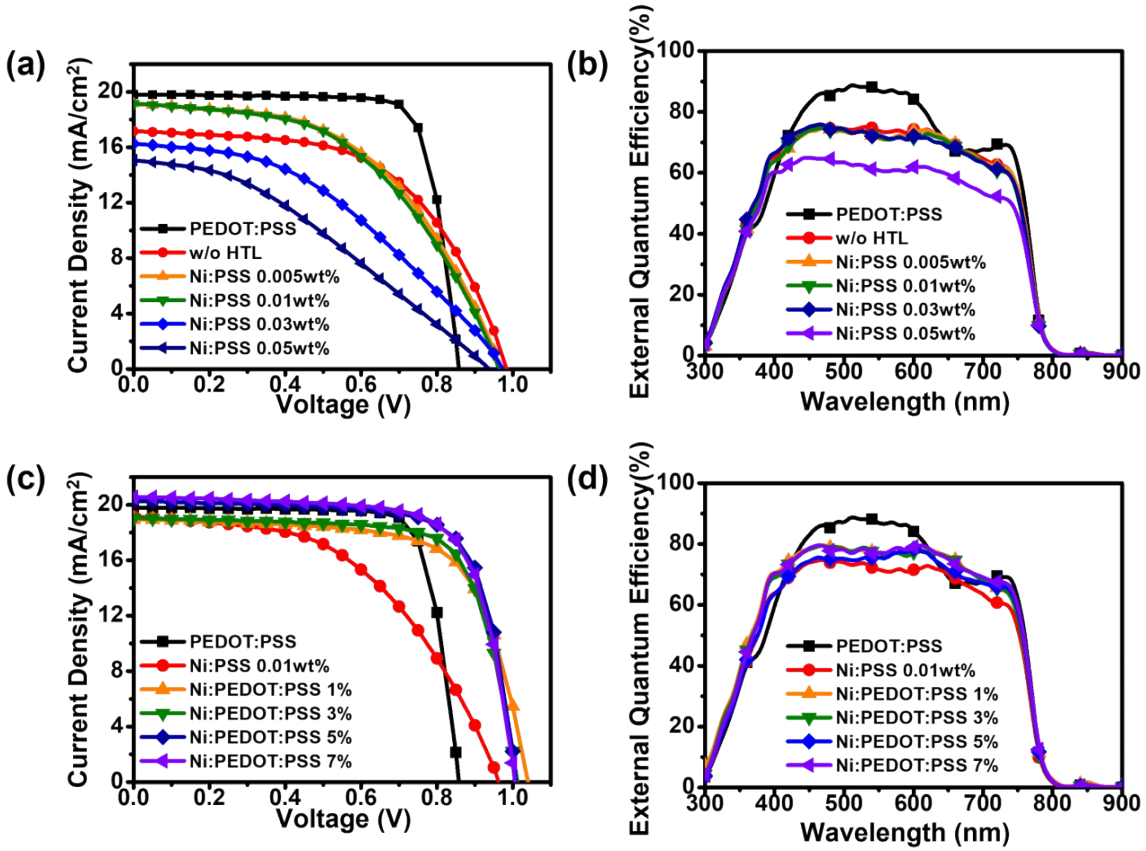

Fig. S1. Device characteristics of perovskite solar cells under illumination using Ni:PSS and Ni:PEDOT:PSS HTLs. (a),(c) J-V characteristics, (b),(d) External quantum efficiency

Table S2. Device characteristics of perovskite solar cells.

Hole transport layer	Thickness (nm)	J_{SC} (mA/cm²)	V_{OC} (V)	FF (%)	PCE (%)
PEDOT:PSS	25.06	19.09 ± 1.15	0.85 ± 0.01	76.97 ± 3.2	12.48 ± 0.89
Ni:PSS 0.005wt%	-	16.55 ± 1.30	0.95 ± 0.05	47.26 ± 3.6	7.44 ± 0.99
Ni:PSS 0.01wt%	0.83	17.83 ± 0.74	0.95 ± 0.04	54.49 ± 4.1	9.28 ± 0.25
Ni:PSS 0.03wt%	-	15.67 ± 1.04	0.93 ± 0.06	36.84 ± 3.9	5.13 ± 0.59
Ni:PSS 0.05wt%	1.79	14.41 ± 1.54	0.85 ± 0.10	27.77 ± 4.4	3.40 ± 0.84
Ni:PEDOT:PSS 1%	1.55	18.28 ± 1.02	1.01 ± 0.01	64.91 ± 3.7	12.02 ± 1.08
Ni:PEDOT:PSS 3%	2.21	19.14 ± 0.94	1.02 ± 0.12	69.62 ± 2.3	13.59 ± 0.62
Ni:PEDOT:PSS 5%	5.33	19.31 ± 0.98	1.01 ± 0.01	72.10 ± 4.0	14.03 ± 0.79
Ni:PEDOT:PSS 7%	12.34	19.55 ± 1.09	0.99 ± 0.01	71.62 ± 3.3	13.91 ± 0.96

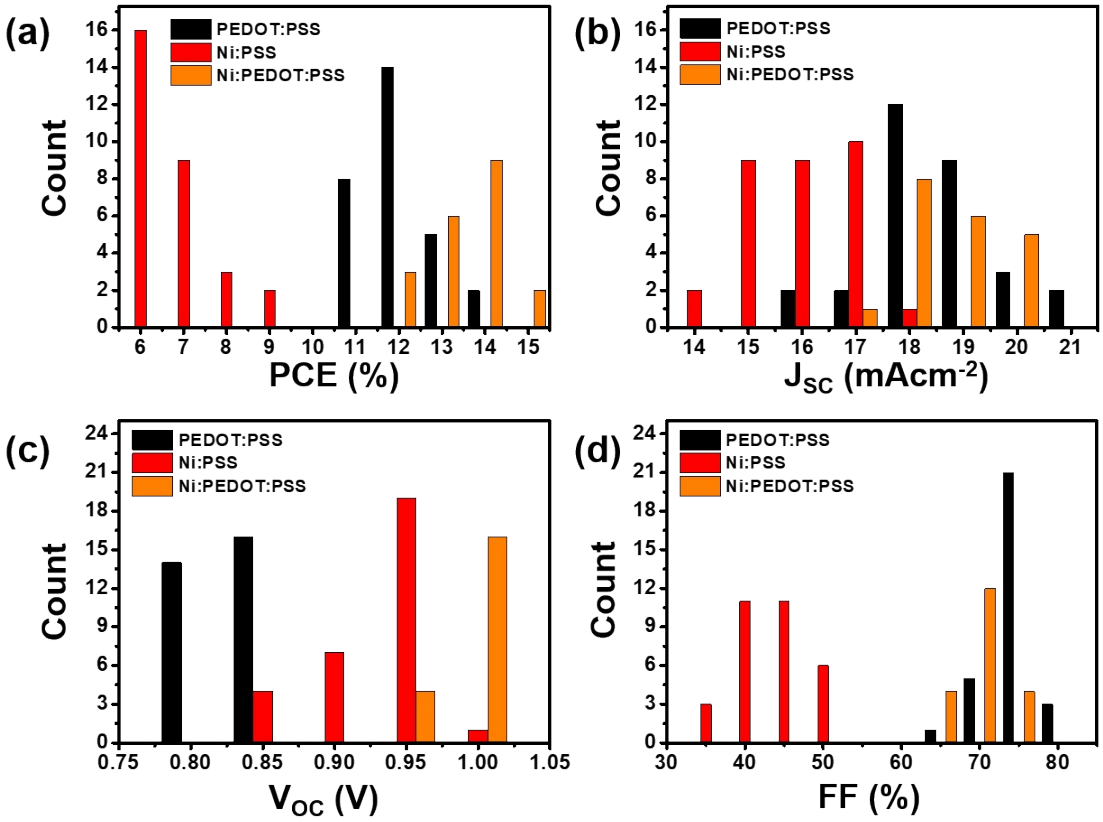

Fig. S2. Perovskite solar cell statistics. Histogram showing (a) distribution of PCE values, (b) distribution of J_{SC} values, (c) distribution of V_{OC} values and (d) distribution of FF values.

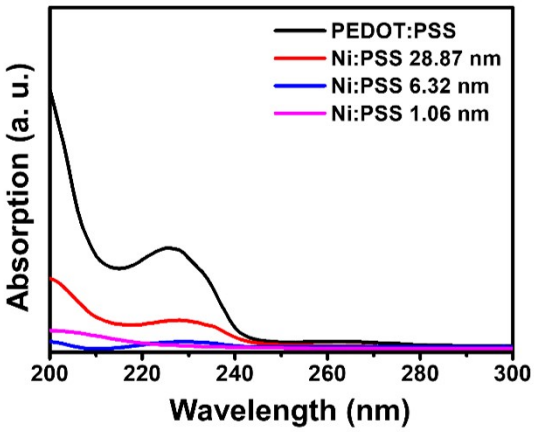

Fig. S3. UV-vis spectroscopy absorption spectrum of Ni:PSS and PEDOT:PSS

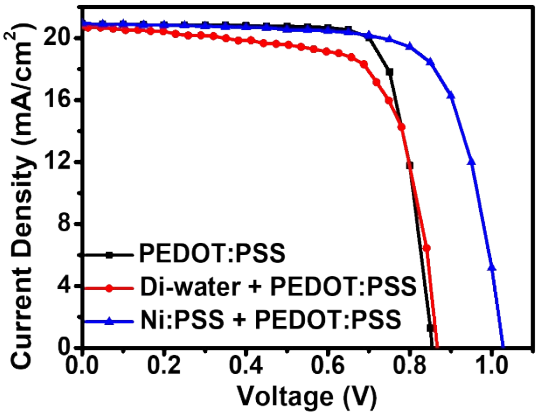

Fig. S4. J-V characteristics of perovskite solar cells under illumination using diluted PEDOT:PSS and Ni:PEDOT:PSS HTLs.

Hole transport layer	J_{SC} (mA/cm^2)	V_{OC} (V)	FF (%)	PCE (%)

PEDOT:PSS	20.91	0.86	78.47	14.02
Di-water + PEDOT:PSS	21.10	0.76	76.67	13.58
Ni:PSS + PEDOT:PSS	20.96	1.03	72.46	15.67

Table S3. Device characteristics of perovskite solar cells using diluted PEDOT:PSS and Ni:PEDOT:PSS .

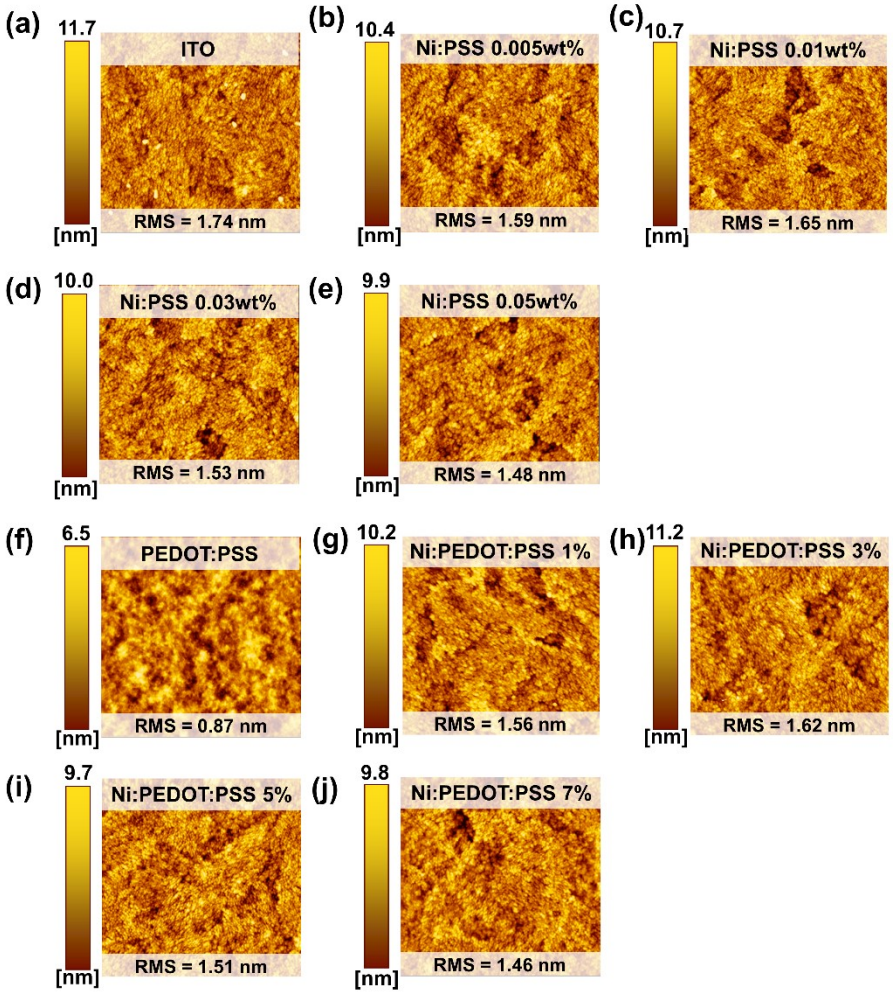

Fig. S5. AFM images of Ni:PSS and Ni:PEDOT:PSS films on ITO substrates. (a)-(e) different thickness of Ni:PSS, (f)-(j) Mixed Ni:PEDOT:PSS films prepared from solutions with different volumes of PEDOT:PSS.

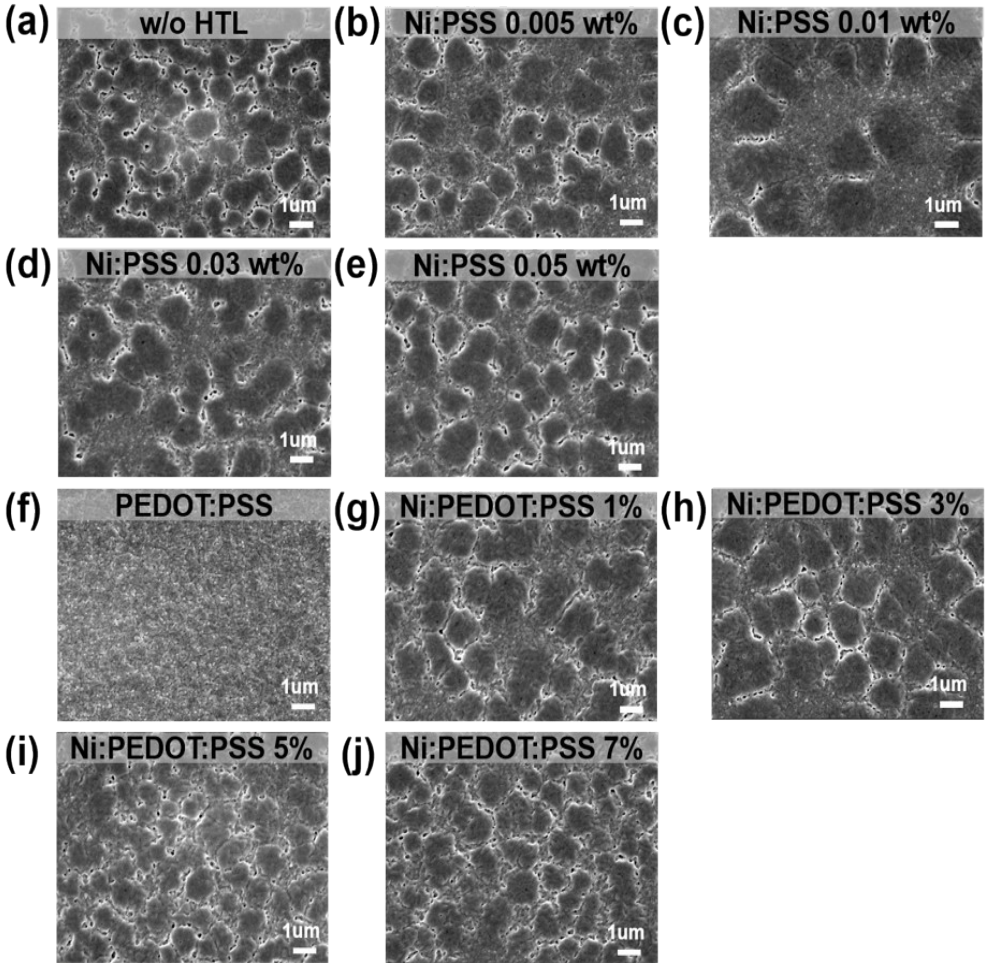

Fig. S6. SEM images of Ni:PSS and Ni:PEDOT:PSS films on ITO substrates. (a)-(e) different thickness of Ni:PSS, (f)-(j) Ni:PSS layer with different volumes of PEDOT:PSS

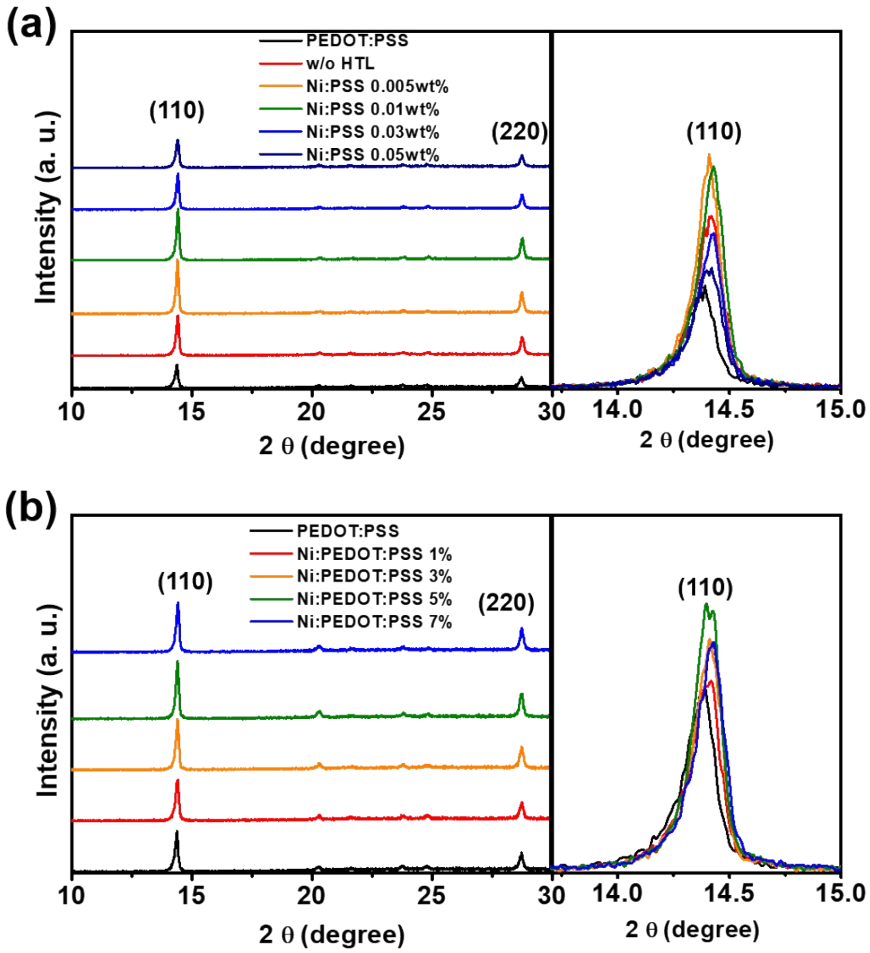

Fig. S7. X-ray diffraction patterns of different HTLs including (a) Ni:PSS films and (b) Ni:PSS films containing PEDOT:PSS as an additive.

Table S4. XRD Parameters of $MAPbI_3$ films deposited on variable HTLs.

Hole transport layer	Peak Position (2θ)	Intensity	FWHM	d-spacing (Å)	Crystal Size (Å)	Grain sizes[1] (μm)
PEDOT:PSS	14.39	811.67	0.1732	6.155	46.259	0.404
w/o HTL	14.42	1351.67	0.1553	6.142	51.596	1.026
Ni:PSS 0.005 wt%	14.41	1841.67	0.1395	6.147	57.413	1.056
Ni:PSS 0.01 wt%	14.43	1743.33	0.1458	6.138	54.954	1.359
Ni:PSS 0.03 wt%	14.43	1218.33	0.1491	6.138	53.742	1.257
Ni:PSS 0.05 wt%	14.42	948.33	0.1604	6.142	49.949	1.290
Ni:PEDOT:PSS 1%	14.42	816.67	0.1673	6.142	47.909	1.378
Ni:PEDOT:PSS 3%	14.41	1006.67	0.1566	6.147	51.173	1.296
Ni:PEDOT:PSS 5%	14.40	1143.33	0.1475	6.151	54.323	1.078

Ni:PEDOT:PSS 7%	14.43	990.00	0.1603	6.138	49.987	1.106

[1] Grain sizes were calculated from the SEM images in Fig. S5 using ImageJ software.

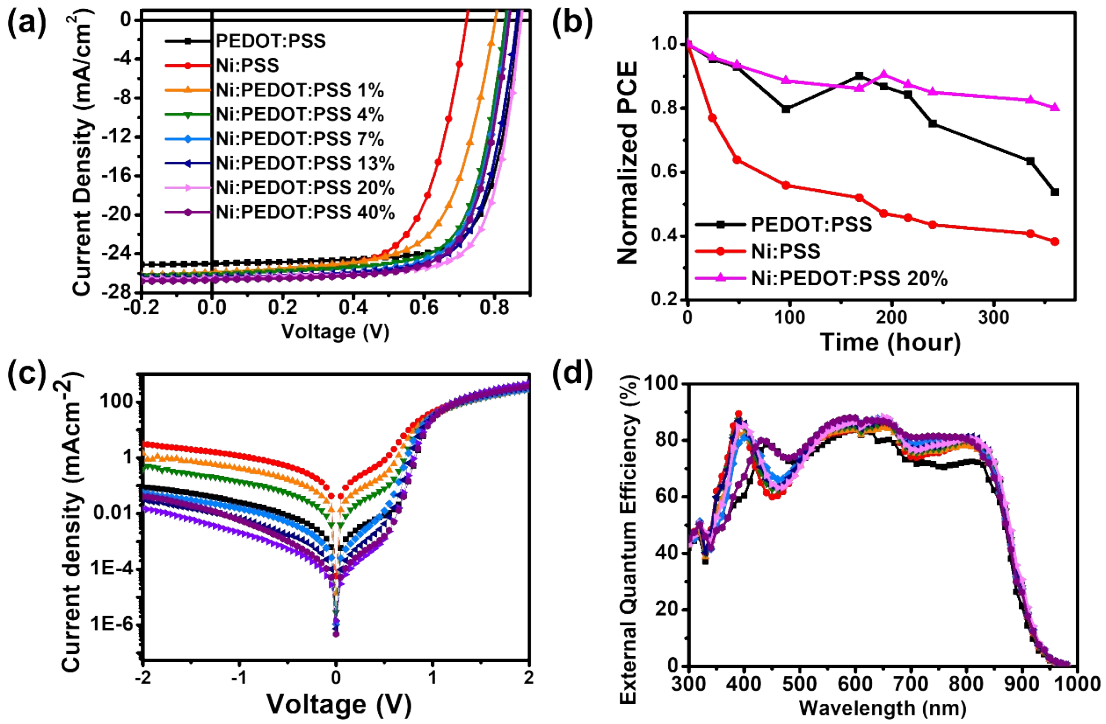

Fig. S8. Device characteristics of of organic (PM6:Y6) solar cells under illumination using Ni:PSS and Ni:PEDOT:PSS HTLs. (a) J-V characteristics, (b) device stability, (c) dark current density, (d) external quantum efficiency.

Table S5. Device characteristics of PM6:Y6 solar cells.

Hole transport layer	Thickness (nm)	J_{SC} (mA/cm^2)	$J_{SC\text{-}EQE}$ (mA/cm^2)	V_{OC} (V)	FF (%)	PCE (%)
PEDOT:PSS	25.06	25.37 ± 0.23	24.35	0.86 ± 0.01	71.20 ± 1.00	15.60 ± 0.12
Ni:PSS	1.79	25.95 ± 0.36	25.35	0.69 ± 0.03	63.40 ± 1.40	11.20 ± 0.65
Ni:PEDOT:PSS 1%	3.09	26.31 ± 0.26	25.21	0.73 ± 0.05	64.50 ± 0.90	12.40 ± 0.75
Ni:PEDOT:PSS 4%	4.49	26.04 ± 0.21	25.67	0.82 ± 0.02	68.80 ± 0.90	14.60 ± 0.41
Ni:PEDOT:PSS 7%	6.02	26.41 ± 0.28	26.02	0.82 ± 0.01	69.40 ± 0.80	15.10 ± 0.44
Ni:PEDOT:PSS 13%	10.09	26.49 ± 0.31	25.99	0.85 ± 0.01	70.50 ± 0.40	15.80 ± 0.27
Ni:PEDOT:PSS 20%	15.23	26.56 ± 0.31	25.98	0.87 ± 0.01	71.80 ± 1.40	16.50 ± 0.25
Ni:PEDOT:PSS 40%	21.69	26.39 ± 0.23	26.23	0.86 ± 0.01	69.20 ± 1.50	15.60 ± 0.26

Table S6. The current-voltage response measured in the dark of PM6:Y6 solar cells.

Hole transport layer	R_{Sh} (kΩ)	R_S (Ω)
PEDOT:PSS	63.613	0.183
Ni:PSS	1.047	0.187
Ni:PEDOT:PSS 1%	3.074	0.187
Ni:PEDOT:PSS 4%	9.944	0.170
Ni:PEDOT:PSS 7%	116.788	0.130
Ni:PEDOT:PSS 13%	294.143	0.142
Ni:PEDOT:PSS 20%	1074.444	0.142
Ni:PEDOT:PSS 40%	630.226	0.149

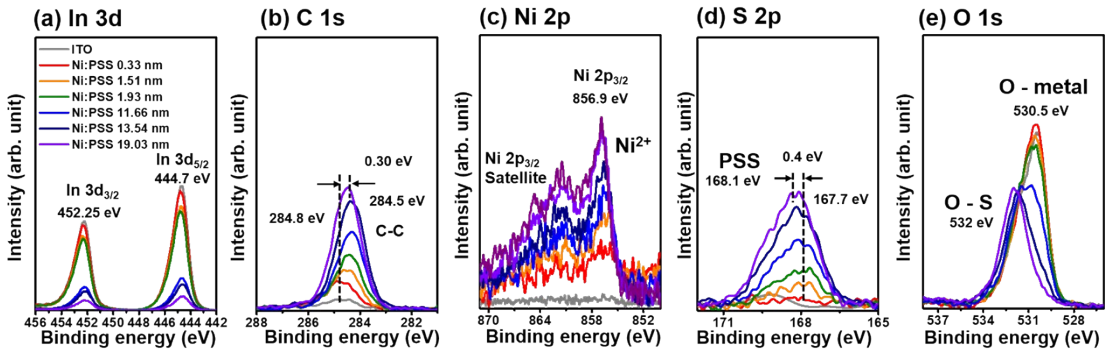

Fig. S9. XPS spectra of Ni:PSS films with variable thickness corresponding to (a) In 3d, (b) C 1s, (c) Ni 2p, (d) S 2p and (e) O 1s.

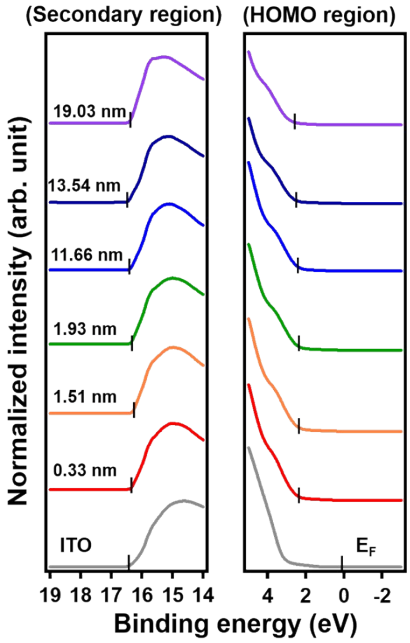

Fig. S10. UPS spectra of Ni:PSS films with variable thickness.

Table S7. Energy levels of Ni:PSS on ITO substrates derived from UPS data.

Substrate	Thickness (nm)	WF (eV)	E_{HOMO} (eV)	EA (eV)	IP (eV)
ITO/Ni:PSS	0	4.74	-	-	-
	0.33	4.85	2.37	2.12	7.22
	1.51	4.88	2.29	2.07	7.17
	1.93	4.83	2.37	2.09	7.19
	11.66	4.80	2.33	2.04	7.14
	13.54	4.73	2.48	2.12	7.22
	19.03	4.79	2.71	2.40	7.50

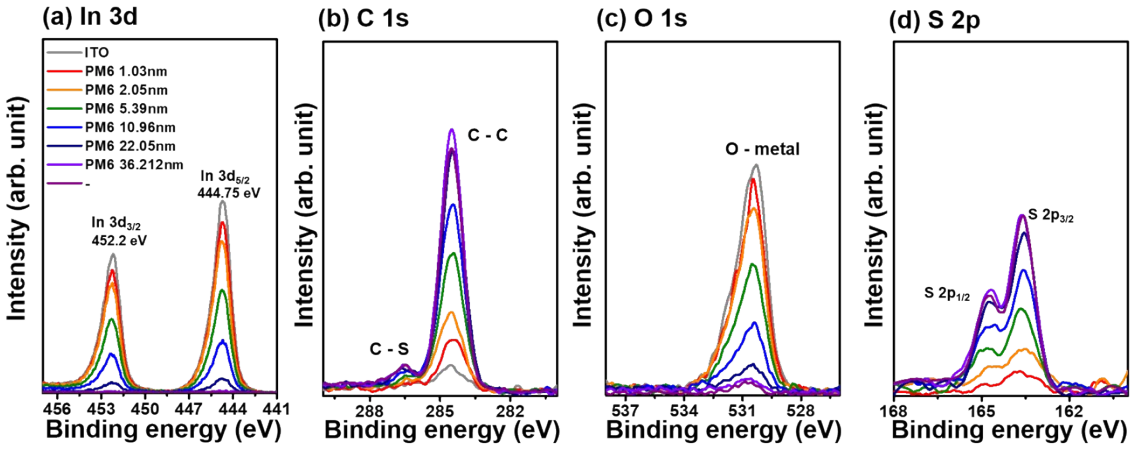

Fig. S11. XPS spectra of ITO/PM6 films with variable thickness corresponding to (a) In 3d, (b) C 1s, (c) O 1s and (d) S 2p.

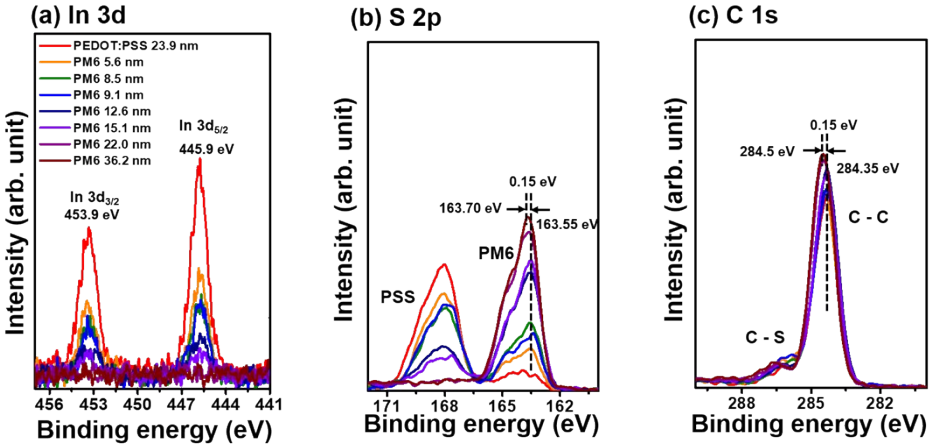

Fig. S12. XPS spectra of PEDOT:PSS/PM6 films with variable thickness corresponding to (a) In 3d, (b) S 2p and (c) C 1s.

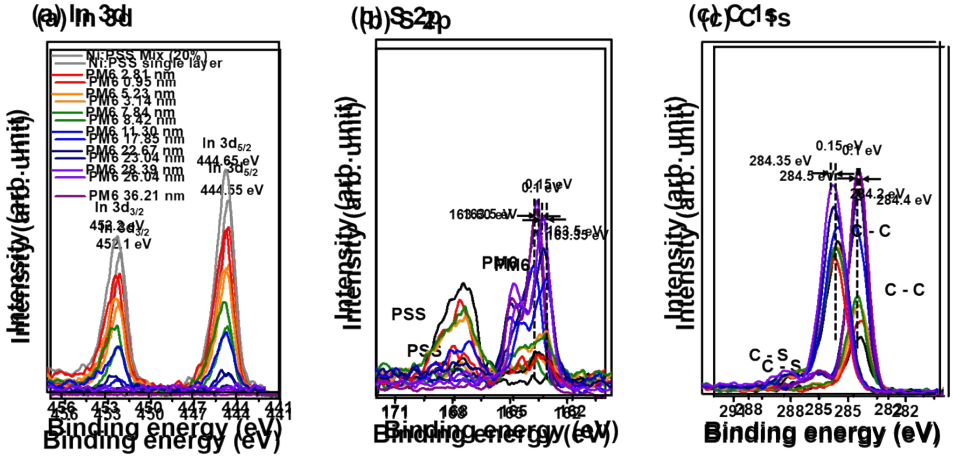

Fig. S13. XPS spectra of Ni:PEDOT:PSS/PM6 films with variable thickness corresponding to (a) In 3d, (b) S 2p and (c) C 1s.

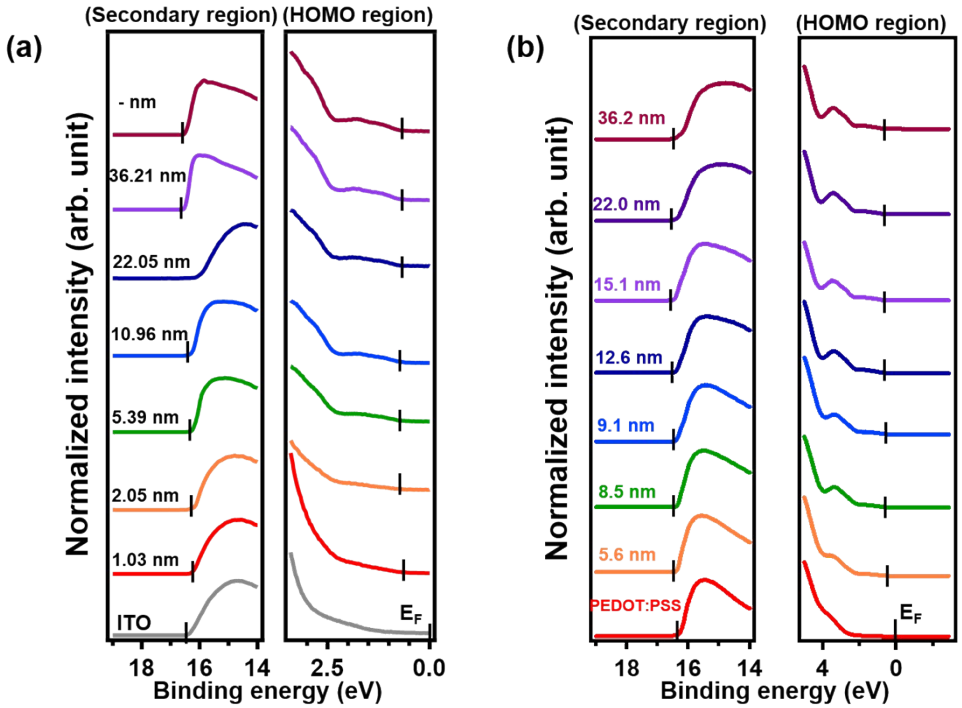

Fig. S15.UPS spectra of PM6 films with variable thickness corresponding to (a) ITO/PM6, and (b) PEDOT:PSS/PM6.

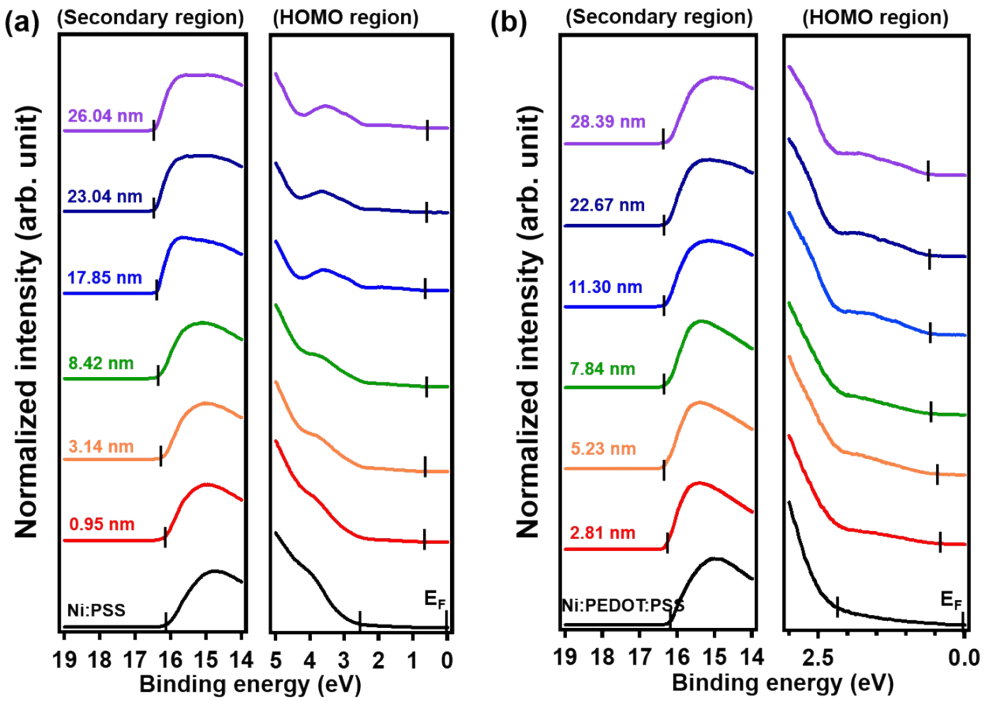

Fig. S16. UPS spectra of PM6 films with variable thickness corresponding to (a) Ni:PSS/PM6, and (b) Ni:PEDOT:PSS/PM6.

Table S8. Energy levels of PM6 deposited on various substrates derived from UPS data.

Substrate	Thickness (nm)	WF (eV)	E_{HOMO} (eV)	EA (eV)	IP (eV)
ITO/PM6	0	4.61	-	-	-
	1.03	4.92	0.59	3.62	5.51
	2.05	4.89	0.67	3.67	5.56
	5.39	4.88	0.66	3.66	5.55
	10.96	4.79	0.68	3.58	5.47
	36.21	4.66	0.67	3.45	5.34
	-	4.67	0.67	3.45	5.34
PEDOT:PSS/PM6	0	4.98	2.59	5.69	7.58
	5.6	4.83	0.36	3.31	5.19
	8.5	4.84	0.41	3.36	5.25
	9.1	4.81	0.43	3.35	5.24
	12.6	4.78	0.51	3.40	5.29
	15.1	4.75	0.53	3.39	5.28
	22.0	4.74	0.53	3.38	5.28
	36.2	4.77	0.58	3.47	5.36
Ni:PSS/PM6	0	5.06	2.81	5.98	7.87
	0.95	4.87	0.72	3.70	5.59
	3.14	4.83	0.69	3.63	5.52
	8.42	4.81	0.67	3.58	5.47
	17.85	4.78	0.61	3.51	5.39
	23.04	4.78	0.59	3.49	5.38
	26.04	4.76	0.59	3.47	5.36
Ni:PEDOT:PSS/PM6	0	4.94	2.38	2.22	7.32
	2.81	4.92	0.45	3.48	5.37
	5.23	4.89	0.49	3.50	5.39
	7.84	4.88	0.55	3.54	5.43
	11.30	4.83	0.57	3.51	5.40
	22.67	4.78	0.60	3.49	5.38
	28.39	4.78	0.61	3.50	5.39

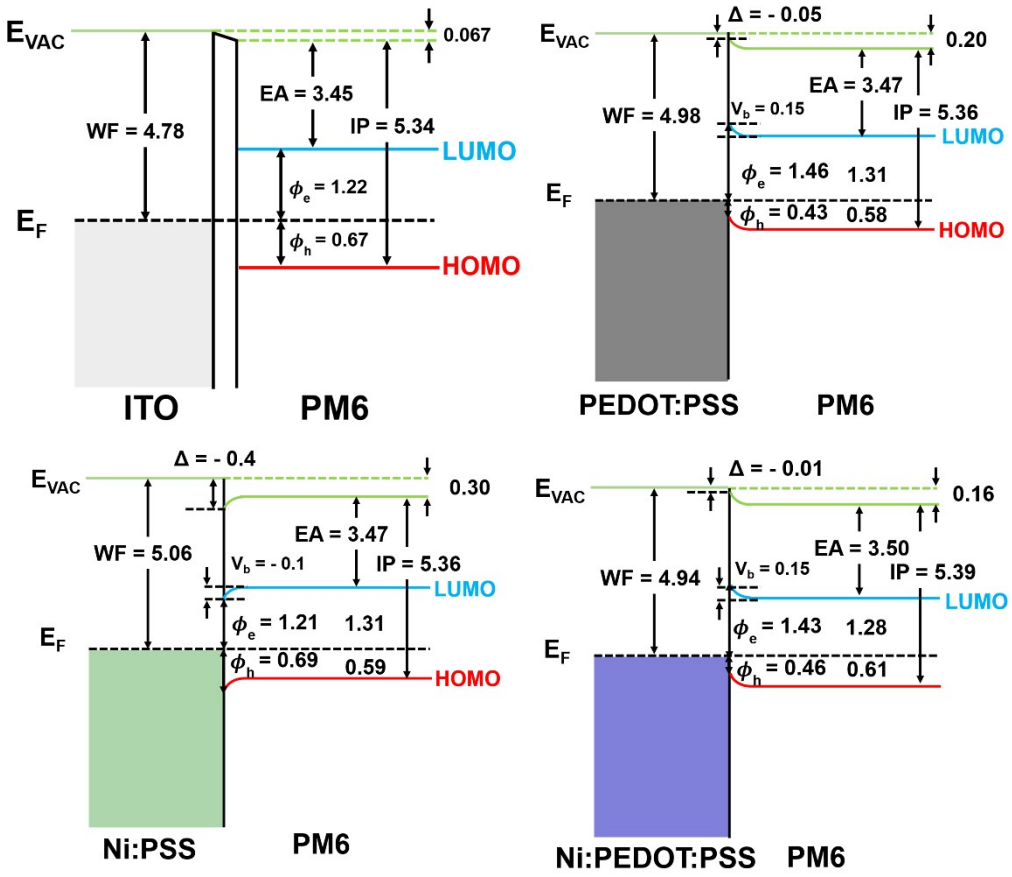

Fig. S17. Band diagram of PM6 depending on the substrate.